Oran 2 University Journal مجلة جامعة وهران 2
e-ISSN : 2716-9448 p-ISSN : 2507-7546
Volume 7 Issue 2 / October 2022 pp. 17-26
[Special Issue] The 1st International Symposium on Industrial Engineering Maintenance and Safety: IEMS'22.
IEMS 2022 Hybrid Mode | 05 - 06 March 2022 | Oran, Algeria.

Dynamic flow behaviour in a Straight T-Bifurcating Channel

Mohammed SAID[1]
Abdelhak LAKEHAL[2]
Nora NAIT BOUDA[3]
Hemiche IDDOU[4]
[1,2,3,4] Laboratoire de Mécanique des Fluides Théorique et Appliquée, Université des Sciences et de la Technologie Houari Boumediene, Alger (Algérie)

Received: 28/04/2022, **Accepted:** 19/10/2022, **Published:** 31/10/2022

Abstract: *This work deals with a two-dimensional (2D) numerical study of a turbulent flow in a rectangular T-bifurcating duct. The configuration refers to the cooling mechanism existent in the stator of the electrical machines. Indeed, radial vents are placed vertically to the rotor-stator airgap to ensure airflow. Therefore, a better understanding of the flow behaviour in the bifurcation is important. The effect of branch aspect ratio is particularly investigated in this purpose. To ensure the closure of the Navier–Stokes equations system governing the turbulent flow in the T-bifurcation we used the first order k-ω SST model. For the different lateral branch widths, the results show the existence of a recirculation zones on the left wall of the branch (in front of the bifurcation) and downstream of the bifurcation. The recirculation zone and the turbulent diffusion are very influenced by the aspect ratio of the side branch.*

Keywords: T-bifurcating, rotor-stator, turbulence, flow structure, recirculation zone.

Résumé : *Ce travail traite d'une étude numérique bidimensionnelle (2D) d'un écoulement turbulent dans un canal rectangulaire à bifurcation en T. La configuration se réfère au mécanisme de refroidissement dans le stator des machines électriques. En effet, des évents radiaux sont placés à la verticale de l'entrefer pour assurer la circulation de l'air. Par conséquent, une meilleure compréhension du comportement de l'écoulement dans la bifurcation est importante. L'effet du rapport d'aspect de la branche est particulièrement étudié dans cet article. Pour assurer la fermeture du système d'équations de Navier-Stokes régissant l'écoulement turbulent dans la bifurcation T, nous avons utilisé le modèle SST k-ω du premier ordre. Pour les différentes largeurs de branches latérales, les résultats montrent l'existence d'une zone de recirculation sur la paroi gauche de la branche (en avant de la bifurcation) et en aval de la bifurcation. La longueur de ces zones et la diffusion turbulente sont très influencées par le rapport d'aspect de la branche latérale.*

Mots-clés : Bifurcation en T, rotor-stator, turbulence, structure de l'écoulement, zone de recirculation.

[1] E-mail : medsaid@usthb.dz
[2] E-mail : lakabdelhak@hotmail.com
[3] E-mail : naitboudanora@gmail.com
[4] E-mail : hemicheiddou95@gmail.com

1. Introduction :

Flow in channels with bifurcation are encountered in many technical applications. They can be used as heating and cooling tools in industry. The research area for this configuration is still under investigation due to the complexity of the resulting flow. Indeed, the sudden change in flow geometry at the bifurcation generates complex phenomena (turbulence, flow separation and recirculation, secondary flow).

In 1987 Bramley and Sloan (Bramley & Sloan, 1987) conducted a numerical study in a semi-infinite channel with a bifurcation. The effects of Reynolds number, deflection angle and channel width on a two-dimensional flow of a viscous, incompressible fluid were studied. The results show that the shape of the angle has a qualitative influence on the flow characteristics. In addition, the size of the recirculation zone increases slightly as the angle of deflection increases.

Paál et al (Paál & Pinho, 2003) studied numerically the flow in a T-junction with a circular cross-section. The turbulence modelling was done by the k-ω SST model and the RSM (Reynolds stress model) with an unstructured mesh. Both models correctly reproduce the mean flow field. However, the RSM model more accurately reproduces the width of the recirculation zone.

In a conference paper presented by Jaroslav Štigler et al (Ŝtigler et al., 2012). The author presented some comparative results from PIV measurements and a CFD simulation investigating whether CFD simulation can successfully reproduces measurements obtained by the PIV. Their results show a remarkable agreement between the PIV measurements and the numerical results.

An experimental and numerical studies of a turbulent flow in a rectangular bifurcating channel were performed by Lakehal and al (Abdelhak et al., 2018)(Lakehal et al., 2017). The dynamic behaviour of the flow and its impact on the convective heat transfer in the branch was investigated. In addition, performance of the RSM model at low Reynolds number were compared to the PIV measurements.

With an aspect ratio of Ar≈11, the researchers noted the weak three-dimensional effects, and suggest that the flow field in the branch can be considered as two-dimensional. Finally, An accelerated flow was observed at the right side of the branch's inlet which could be beneficial for the heat transfer.

In the same interest, the present 2D flow simulation in T-branch channels is done to investigate the effect of branch aspect ratio on the dynamic behaviour of the flow.

It's commonly known that for channel with an aspect ratio exceeding 10, le flow is considered two-dimensional.

2. Description of the flow configuration:

The geometry of the considered T-bifurcating channel and its dimensions are presented in Fig 1. Four zones can be identified: the inlet zone, bifurcating zone, bifurcating branch and outlet zone. It's worth mentioning that the inlet and outlet zones are sufficiently longer to ensure the flow development.

3. Theoretical formulation:

3.1 Flow equations:

Turbulent fluid flow is governed by the RANS Navier-Stokes equations expressing the conservations laws. For an incompressible, Newtonian fluid flowing in a steady state, the conservation equations are written as follows:

Continuity equation:

$$\frac{\partial \overline{u_i}}{\partial x_i} = 0 \qquad 1$$

Momentum equation:

$$\overline{u_j}\frac{\partial \overline{u_i}}{\partial x_j} = -\frac{1}{\rho}\frac{\partial \bar{P}}{\partial x_i} + \frac{\partial}{\partial x_j}\left[\frac{\mu}{\rho}\frac{\partial \overline{u_i}}{x_j} - \overline{u_i' u_j'}\right] \qquad 2$$

With $\overline{u_i' u_j'}$, ν, ρ are respectively the Reynolds stresses, kinematic viscosity and density.

4. Turbulence modelling:

4.1 The SST k-ω model:

The SST k-ω model is a two equation turbulence model that is used for many hydrodynamic applications. It's a hybrid model combining the Wilcox k-ε model and k-ω model (Wilcox, n.d.).

a. SST k-ω Governing equations:

Turbulence kinetic energy:

$$\frac{\partial k}{\partial t} + U_j \frac{\partial k}{\partial x_j} = P_k - \beta^* k\omega + \frac{\partial}{\partial x_j}\left[(\nu + \sigma_k \nu_T)\frac{\partial k}{\partial x_j}\right] \quad 3$$

Specific dissipation rate:

$$\frac{\partial \omega}{\partial t} + U_j \frac{\partial \omega}{\partial x_j} = \alpha S^2 - \beta\omega^2 + \frac{\partial}{\partial x_j}\left[(\nu + \sigma_\omega \nu_T)\frac{\partial \omega}{\partial x_j}\right] + 2(1 - F_1)\sigma_{\omega 2}\frac{1}{\omega}\frac{\partial k}{\partial x_i}\frac{\partial \omega}{\partial x_i} \quad 4$$

Or F_1 is a Blending function.

$$F_1 = \tanh\left\{\left\{min\left[max\left(\frac{\sqrt{k}}{\beta^*\omega y}, \frac{500\nu}{y^2\omega}\right), \frac{4\sigma_{\omega 2}k}{CD_{k\omega}y^2}\right]\right\}^4\right\} \quad 5$$

F_1=1 inside the boundary layer and 0 in the free stream.

$$CD_{k\omega} = max\left(2\rho\sigma_{\omega 2}\frac{1}{\omega}\frac{\partial k}{\partial x_i}\frac{\partial \omega}{\partial x_i}, 10^{-10}\right) \quad 6$$

Kinetic eddy viscosity:

$$\nu_T = \frac{\alpha_1 k}{max(a_1\omega, SF_2)} \quad 7$$

F_2 is the second blending function.

$$F_2 = \tanh\left[\left[max\left(\frac{2\sqrt{k}}{\beta^*\omega y}, \frac{500\nu}{y^2\omega}\right)\right]^2\right] \quad 8$$

P_k is the production limiter.

$$P_k = min\left(\tau_{ij}\frac{\partial U_i}{\partial x_j}, 10\beta^* k\omega\right) \quad 9$$

The following table presents the k-ω SST model constants:

Table 1: k-ω SST model constants.

Constant	α	α_1	α*	β	β*	σ_k	β2	σ_ω	$\sigma_{\omega 2}$
Value	0.52	0.31	1	0.075	0.09	0.85	0.0828	0.5	0.856

4.2 Boundary Conditions:

At the entrance of the computational domain, a parabolic velocity profile is introduced through an UDF (User defined function). The turbulence intensity is calculated according to the following expression:

$$I_0 = 16\left(Re_{D_h}\right)^{1/8} \quad 10$$

The hydraulic diameter of the inlet channel , $D_h = 35.8$ mm. The Reynolds number based on the inlet bulk velocity U_0 and the hydraulic diameter D_h, $Re_{D_h} = 36000$ and Re_{Dh}= 30000.

Taking into account the assumption of mass flow conservation, we imposed different flow rates for each outlet. A flow rate ratio of $\psi_2 = Q_{outII}/Q_{in}$= 22% and $\psi_1 = Q_{outII}/Q_{in}$= 73% was used in this study. Q_{in}, Q_{out_I}, $Q_{out_{II}}$ are shown in figure 1.

All walls were declared as a non-slip boundary conditions.

Figure 1: Schematic of the geometry and the grid mesh

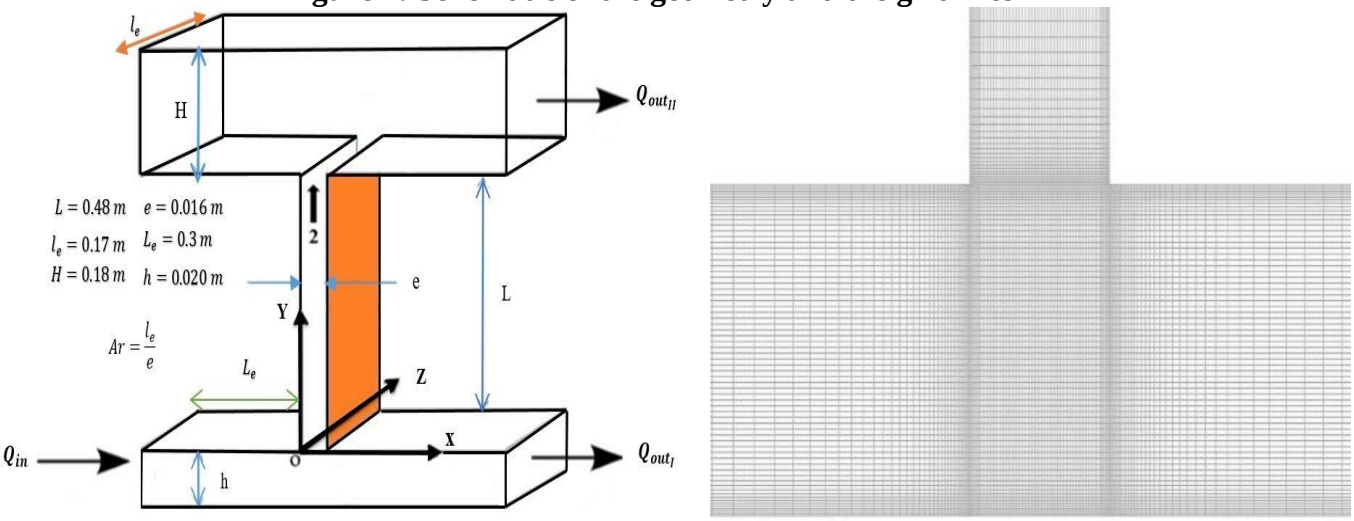

4.3 Numerical procedure:

The simulations were performed with the Commercial Software ANSYS Fluent, which is based on the finite volume technique. We present on Figure 1 the grid in the bifurcation area where a mesh refinement is introduced near each wall to reflect the steep gradients in this region.

The momentum equation, k and ω were discretised with a second order UPWIND scheme while for the pressure the Standard scheme was used. The velocity pressure coupling is performed using SIMPLE algorithm.

Double precision was used for all calculations. Besides, the equations were considered to be converged when the absolute values of the residuals were 10^{-4}.

A mesh independency study was carried out with three different meshes (coarse, medium, fine) as shown in Table 1. The independency test shows almost the same results in terms of velocity profile before the junction and the side branch.

The influence of grid refinement near the walls was also investigated. The size of the first cell at the wall is about 10^{-5} m, which gives a satisfactory results.

Table 2: Details of grids used in the mesh-independence tests.

	Inlet Region		Junction Region		Outlet Region I		Outlet Region II	
	Nx	Ny	Nx	Ny	Nx	Ny	Nx	Ny
Grid I	150	50	50	50	350	50	50	300
Grid II	150	70	65	70	350	70	65	300
Grid III	150	90	85	90	350	90	85	300

5. RESAULTS AND DESCUSSION:

5.1 Dimensionless parameters:

For the analyses and treatment of the results, dimensionless numbers must be defined. The characteristic length for the Reynolds number and for the normalization is the hydraulic diameter of the inlet channel with D_h= 0.0358 m.

$$X = \frac{x}{e};\ Y = \frac{y}{h};\ V = \frac{\bar{v}}{V_0};\ Ar = \frac{l_e}{e}$$

V_0, e, h are the bulk velocity at the entrance of the bifurcating channels, the width of the bifurcating and the main channels respectively.

5.2 Validation:

In figure 3, we present the evolution of the normalized mean y-velocity profile at different sections in the lateral branch as designated in figure 2. The SST k-ω results are in good agreement with those obtained by Lakehal et al. (Lakehal et al., 2018) with the RSM model and the PIV measurements.

Figure 3: the evolution of the normalised mean y-velocity profile in the branch.

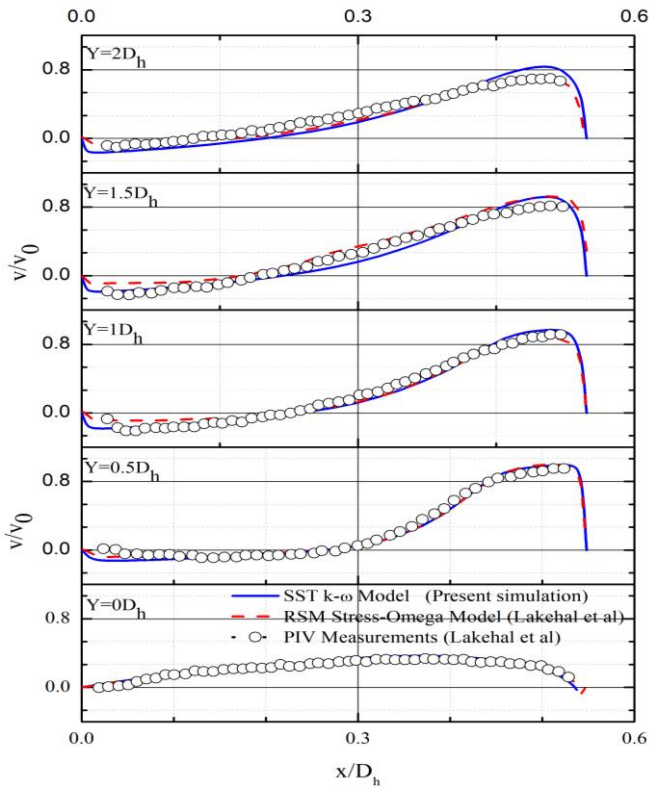

Figure 2: The test sections locations.

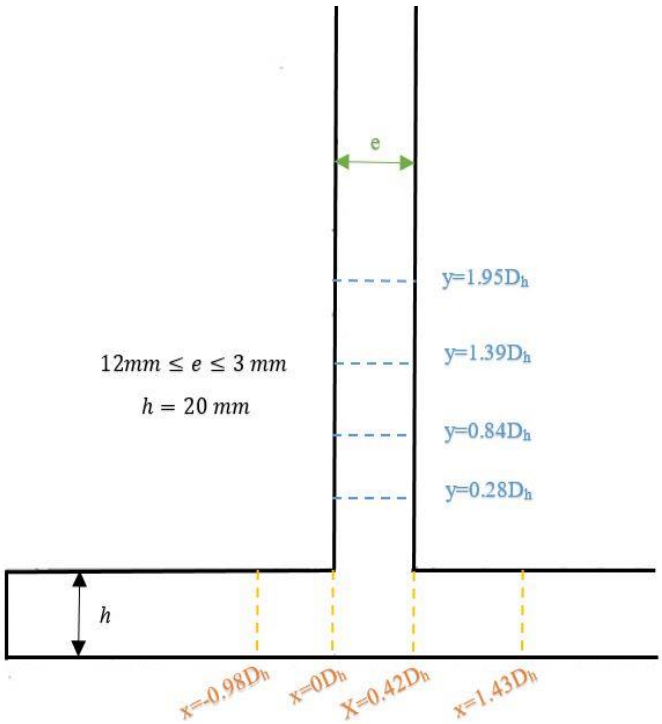

5.3 Mean flow characterization in the branch channel:

In this section, an overview of the flow field in the branch and at the entrance to the bifurcation is presented for different flow ratios ψ and aspect ratios Ar. More details on the input parameters are presented in the table below.

Table 3: input parameters used in this study.

Case	Q_{in} (l/s)	U_0 (m/s)	Outlet	Repartition	$\psi = Q_{II}/Q_{in}$
ψ_1	40.8	12	Haut	73%	0.73
			bas	27%	
ψ_2	63.24	18.6	Haut	22%	0.22
			bas	78%	

Figures 4 and 5 show the magnitude velocity contours and streamlines for two flow ratios and different aspect ratios.

The recirculation zone in the left wall of the branch can be clearly identified for both flow ratios. However, a second recirculation zone is located on the bottom wall of the main channel for ψ_1=0.73.

It is worth mentioning that the size and shape of this zone depends on the flow ratio; short and thin for ψ_1 compared to the second flow ratio ψ_2.

In addition, the effect of Ar on the size and shape of the recirculation zone can also be observed. as Ar increases, the recirculation zone becomes thinner and shorter. however, the recirculation zone present in the main channel does not seem to be significantly affected by the change in aspect ratio Ar.

Figure 4: The streamlines and velocity magnitude at the bifurcating region for different aspect ratios.
Ψ_1=0.73

Ar= 14 **Ar= 24** **Ar= 34**

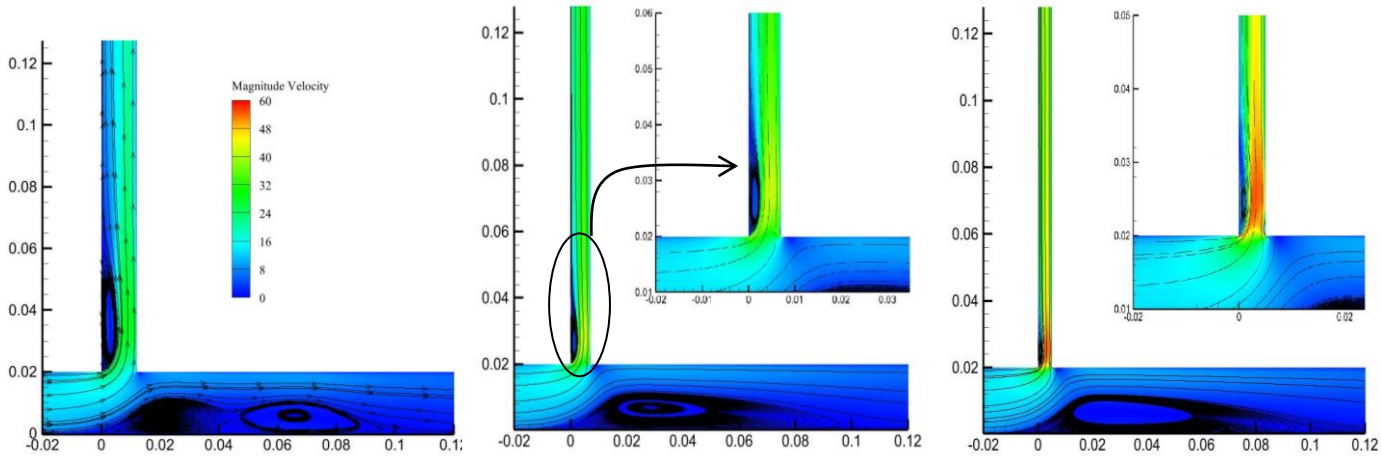

Figure 5: The streamlines and velocity magnitude at the bifurcating region for different aspect ratios.
Ψ_2=0.22

Ar= 14 **Ar=24** **Ar=34**

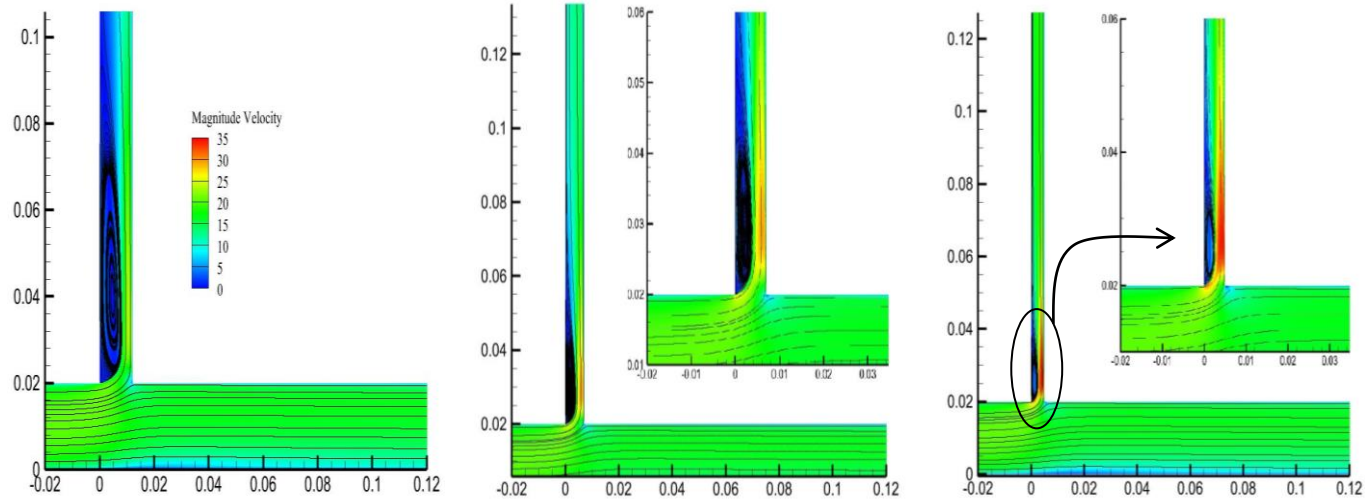

For the flow structure, a significant decrease in flow rate is noticed in the branch when moving from the first flow ratio ψ_1 to the second ψ_2.

For ψ_1 where the major part of the fluid is sucked in through the high outlet. Besides, a relatively high velocity than the inlet velocity was observed on the right side of the branch. this velocity increases significantly with increasing aspect ratio Ar.

On the other hand, on the left side of the branch, a region of low velocities was observed, which proves the existence of a recirculation zone. This recirculation zone is the main cause of the fluid acceleration in the right side of the branch.

In the main channel and just after the bifurcation a second recirculation zone is observed. This recirculation zone is caused by the strong aspiration imposed at the inlet of the lateral branch (Abdelhak et al., 2018).
For the ψ2, the deflected flow is more constricted than for ψ1. this results in more intense shear between the dead fluid and the diverted fluid. by increasing the aspect ratio, the magnitude velocity in the diverted flow also increases.
In the following, we continue this study with the first flow rate ψ_1.
In order to see the evolution of the recirculation length for different aspect ratios, the skin friction coefficient at the left wall of the branch was plotted. The skin friction coefficient Cf is defined as:

$$Cf = \frac{\tau_w}{1/_2 \rho V_0^2} \qquad 11$$

Or τ_w is the wall shear stress, while V_0^2 is the bulk velocity at the entrance branch.
Figure 6 shows the evolution of the friction coefficient in the left wall of the branch. For all aspect ratios, the Cf is negative at the branch entrance. this indicates the existence of a separation zone (recirculation zone) characterised by a negative velocity gradient in this region.
As the flow advances, the Cf increases before changing its sign at a specific distance. This marks the re-collection of the flow and the end of the recirculation zone.
For this purpose, the evolution of the length of the recirculation zone for each aspect ratio can be determined as shown in figure 7. the length of the recirculation zone decreases with increasing aspect ratio *Ar*.

Figure 7 : Evolution of the recirculation zone as a function of aspect ratio Ar.

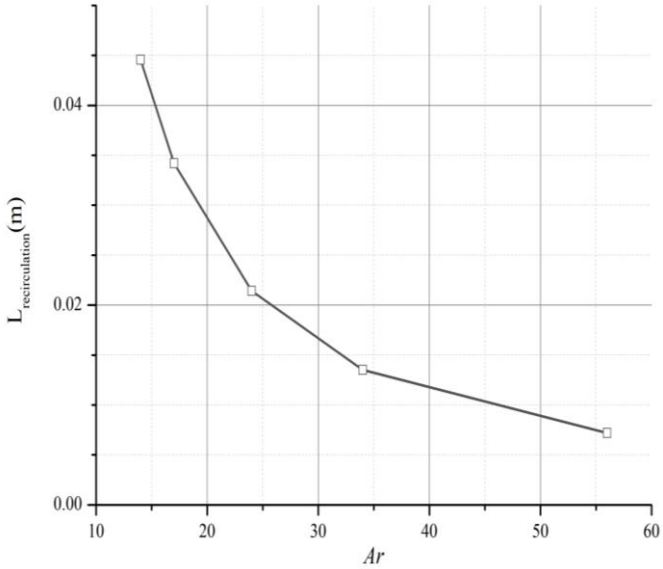

Figure 6: Evolution of the friction coefficient in the left wall of the branch.

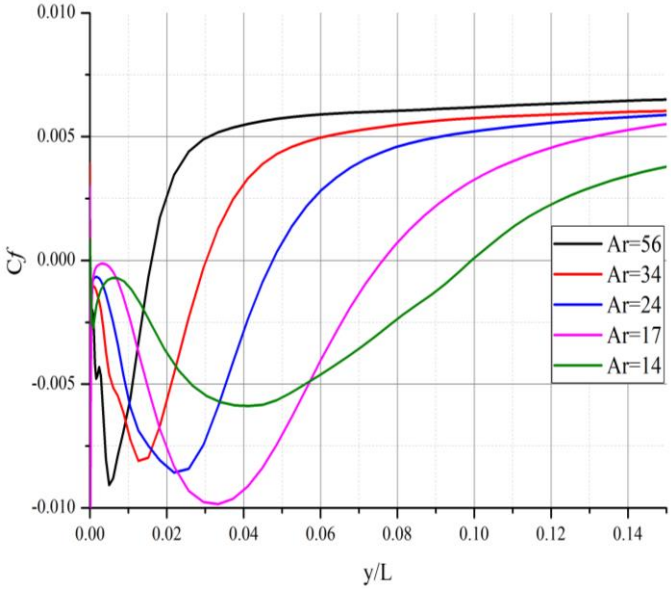

For a $Ar = 56$, the length of the recirculation zone is about $7\ mm$, this length becomes $\sim 13.5\ mm$ for $Ar = 34$. The maximum length of the recirculation zone is $43\ mm$ and was observed for an aspect ratio of $Ar = 14$.

5.4 Turbulent flow characterization in the lateral branch:

The figure 8 shows the normalized turbulent kinetic energy k/V_0^2 profiles in the lateral branch for different aspect ratios. This quantity makes it possible to identify the shear zones; those are due to the interaction of the flow with the right wall of the branch and the recirculation zone. This explains the peak observed at the right wall of the lateral branch.

On the other hand, for $\mathrm{Ar} = 14$, a zone with high k/V_0^2 is located on the right wall and especially near the middle of the branch entrance due to the high partial shear caused by the narrowing of the effective cross-section.

This area is more important at the branch entrance and then decreases along the branch. This shows that the flow starts developing away from the bifurcation.

By increasing the aspect ratio Ar and at the branch entrance, the maximum moves towards the left wall, which proves the narrowing of the recirculation zone. However, beyond an $\mathrm{Ar} = 24$, the turbulent kinetic energy starts to decrease remarkably. This shows the decrease of the turbulent zones at the entrance of the branch.

As we move down the branch, we can clearly observe the effect of aspect ratio. An increase in aspect ratio leads to a decrease in mixing and an attenuation of the turbulent character of the flow.

Figure 9 shows the y-velocity profiles along the side branch for different aspect ratios Ar.

At the branch inlet, for y=0.28D_h a negative velocity zone is located to the left of the branch wall. this indicates the presence of a recirculation zone in this region.

In contrast, on right side, an acceleration of the flow caused by the presence of the recirculation zone is observed. This explains the high velocity in this region. As we move down the branch, and on the left, we notice the disappearance of the negative velocities which indicates that we are out of the recirculation zone.

By increasing the aspect ratio, and at the entrance of the branch, we notice the decrease of the area where the velocities are negative, which indicates the shrinking of the recirculation zone. However, for $Ar = 56$, the negative velocities no longer exist, which indicates that we are outside the recirculation zone.

As we move along the branch, we can observe that the velocity profile starts to develop for *Ar=34* and *Ar=56*. Moreover, the presence of the recirculation zone can be seen for $Ar = 14$, whereas for the other Ar we are already outside this zone.

Figure 9: Evolution of the longitudinal velocity in the branch.

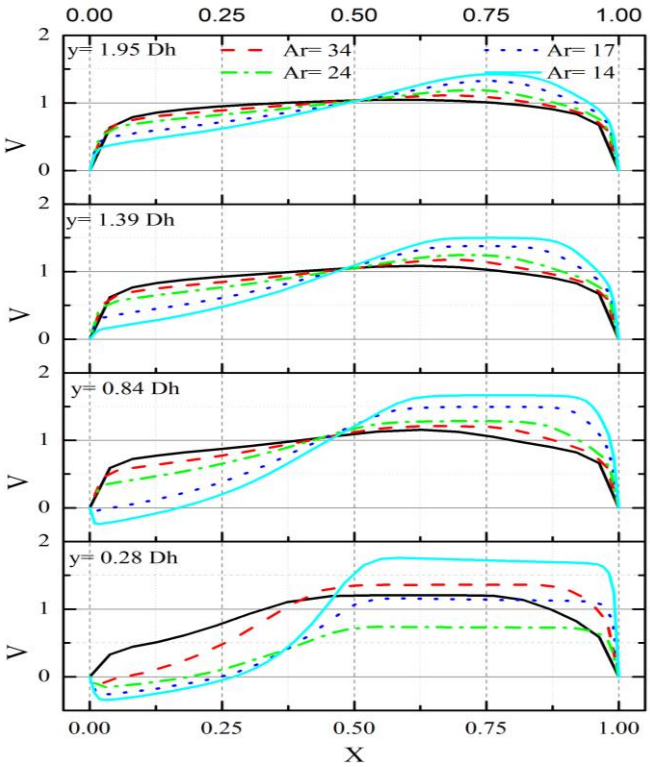

Figure 8: Evolution of the turbulent kinetic energy in the branch.

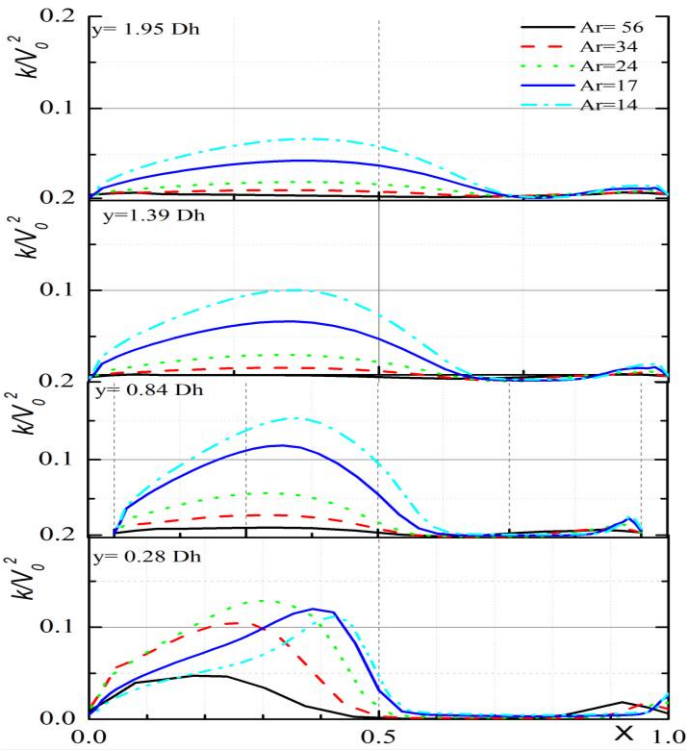

Figure 10 shows The evolution of the turbulent viscosity as a function of aspect ratio **Ar** at various positions.
For aspect ratio $Ar = 14$ and at y=0.28D_h, the turbulent viscosity is significant at the left of the branch wall. This indicates the diffusive aspect of the vortex structures (fluctuating flow) and that the molecular diffusion is masked by the turbulent diffusion.
As we move through the branch, this amount remains high. This is due to the recirculation zone which is, in this case, the seat of diffusive phenomena.
As the aspect ratio is increased, there is no clear difference at the branch entrance due to the presence of the recirculation zone. However, as the branch progresses, the diffusive phenomena start to decrease as the aspect ratio is increased. this proves that we are out of the recirculation zone and that the flow is starting to stabilise.

Figure 10: Evolution of the turbulent viscosity on the lateral branch.

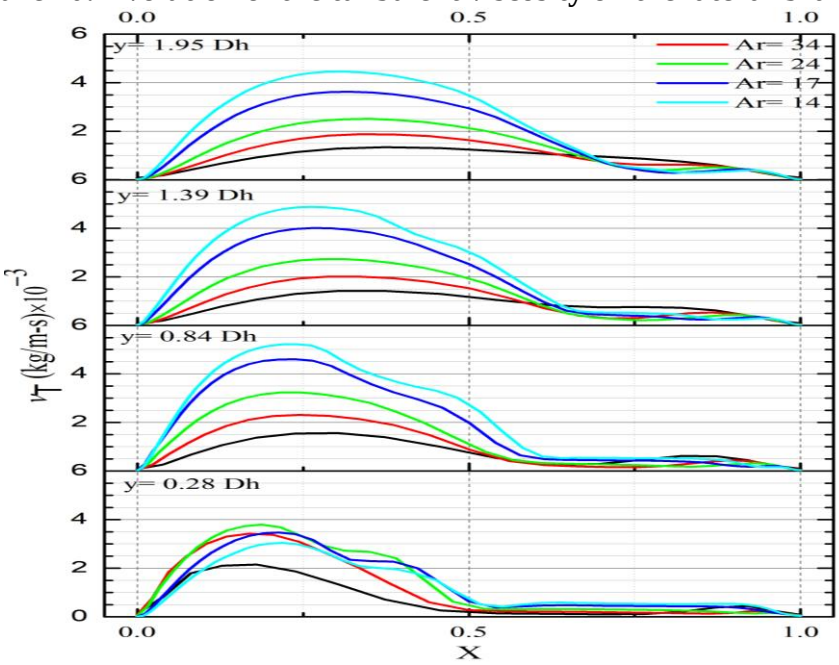

In general, the turbulent nature of the flow present at the inlet and throughout the branch is an important factor affecting heat transfer.
We have seen that the recirculation zone and its size (shape, length) greatly affects the flow behaviour within the branch. Choosing the right flow ratio, and aspect ratio would be essential to maximise heat transfer in rotor-stator system.

6. CONCLUSION:

A two-dimensional (2D) numerical study of a turbulent flow in a rectangular T-bifurcating channel was carried out.
The k-ω SST turbulent model was used to study the impact and effect of the aspect ratio on the dynamic behaviour of the flow and its performance was evaluated.
The results obtained with this model are in good agreement with the numerical and experimental results of Lakehal et al (Abdelhak et al., 2018).
The structure and behaviour of the flow in the bifurcation channel has been evolved for two flow ratios and different aspect ratios.

A strong acceleration of the fluid was observed at the entrance of the bifurcation channel caused by the presence of the recirculation zone in the opposite side. The development of this zone is affected by the change of flow ratio ψ and aspect ratio *Ar*.
The turbulent kinetic energy decreases with increasing the aspect ratio, while for the turbulent viscosity and the length of the recirculation zone, the results show a decrease of these two parameters while increasing the aspect ratio *Ar*.
Finally, and for the research perspectives, we suggest a thermal study of the effect of increasing the aspect ratio on the heat transfer and Nusselt number.

7. References:

Abdelhak, L., Nora, N. B., Julien, P., & Souad, H. (2018). On convective heat transfer and flow dynamics through a straight t-bifurcating channel. *Journal of Heat Transfer*, *140*(3). https://doi.org/10.1115/1.4037208

Bramley, J. S., & Sloan, D. M. (1987). Numerical solution for two-dimensional flow in a branching channel using boundary-fitted coordinates. *Computers and Fluids*, *15*(3), 297–311. https://doi.org/10.1016/0045-7930(87)90012-0

Lakehal, A., Nait Bouda, N., & Harmand, S. (2017). Numerical study of convective heat transfer in T-bifurcating channel. *Heat Transfer - Asian Research*, *46*(8), 1262–1280. https://doi.org/10.1002/htj.21272

Paál, G., & Pinho, F. T. (2003). *Numerical predictions of turbulent flow in a 90° tee junction*. *January*.

Ŝtigler, J., Klas, R., Kotek, M., & Kopecký, V. (2012). The fluid flow in the t-junction. The comparison of the numerical modeling and piv measurement. *Procedia Engineering*, *39*, 19–27. https://doi.org/10.1016/j.proeng.2012.07.003

Wilcox, D. C. (n.d.). *by*.